Crossover effects in the random-exchange spin-$\frac{1}{2}$ antiferromagnetic chain

Nicolas Laflorencie,[1] Heiko Rieger,[2] Anders W. Sandvik,[3] and Patrik Henelius[4]
[1]*Laboratoire de Physique Théorique, CNRS-UMR5152 Université Paul Sabatier, F-31062 Toulouse, France*
[2]*Theoretische Physik, Universität des Saarlandes, 66041 Saarbrücken, Germany*
[3]*Department of Physics, Åbo Akademi University, Porthansgatan 3, FIN-20500 Turku, Finland*
[4]*Condensed Matter Theory, Physics Department, KTH, SE-106 91 Stockholm, Sweden*
(Received 22 December 2003; published 31 August 2004)

The random antiferromagnetic spin-1/2 XX and XXZ chain is studied numerically for varying strength of the disorder, using exact diagonalization and stochastic series expansion methods. The spin-spin correlation function as well as the stiffness display a clear crossover from the pure behavior (no disorder) to the infinite randomness fixed point or random singlet behavior predicted by the real space renormalization group. The crossover length scale is shown to diverge as $\xi \sim \mathcal{D}^{-\gamma}$, where $\mathcal{D}$ is the variance of the random bonds. Our estimates for the exponent γ agrees well within the error bars with the one for the localization length exponent emerging within an analytical bosonization calculation. Exact diagonalization and stochastic series expansion results for the string correlation function are also presented.

DOI: 10.1103/PhysRevB.70.054430 PACS number(s): 75.10.Pq, 75.40.Mg, 75.10.Nr, 75.40.Cx

I. INTRODUCTION

Quantum spin chains exhibit a number of interesting features, especially at low temperature when quantum fluctuations are stronger than thermal ones. The antiferromagnetic (AF) Heisenberg model in one dimension (1D) has been extensively studied since the discovery in 1931 of the Bethe ansatz[1] for the spin $S=\frac{1}{2}$ chain. In 1D, the AF XXZ model defined by the Hamiltonian

$$\mathcal{H}^{XXZ} = J\sum_{i=1}^{L} [S_i^x S_{i+1}^x + S_i^y S_{i+1}^y + \Delta S_i^z S_{i+1}^z] \tag{1}$$

with $J>0$, exhibits a gapless excitation spectrum for $\Delta \in [-1,1]$ for $S=\frac{1}{2}$ (and more generally for half integer spins[2]), whereas a gap opens up in the spectrum for integer spins.[3] In 1D, the quantum fluctuations prevent the formation of long-range order[4] but the correlation length of the model [Eq. (1)] is infinite and a *quasi*-long-range order emerges, with power-law decaying spin-spin correlation functions in the ground state (GS),

$$C^{\alpha}(r) = \langle S_i^{\alpha} S_{i+r}^{\alpha} \rangle_{\mathrm{GS}} \propto \frac{(-1)^r}{r^{\eta_\alpha}} \quad \text{for } r \to \infty, \tag{2}$$

where $\alpha = x$, y or z, $\langle \cdots \rangle_{\mathrm{GS}}$ is the GS expectation value, and the critical exponent $\eta_{x,y} = \eta_z^{-1} = 1 - \mu/\pi$, with $\mu = \arccos \Delta$.

If the AF exchange couplings are position-dependent, or more generally distributed randomly according to a probability distribution $\mathcal{P}(J)$, the situation changes dramatically. Indeed, the spin-$\frac{1}{2}$ chain described by the random-exchange XXZ Hamiltonian

$$\mathcal{H}^{XXZ}_{\mathrm{random}} = \sum_{i=1}^{L} [J_\perp(i)(S_i^x S_{i+1}^x + S_i^y S_{i+1}^y) + J_z(i)\Delta S_i^z S_{i+1}^z], \tag{3}$$

has lost the translation symmetry and rare events in the chain dominate the low energy physics.[5,7] Note that the energy scale is set to unity by choosing mean values of random couplings equal to one. Examples of random spin chains include (i) the *random planar exchange* model with $J_z(i)=1$, $\forall i$ and $J_\perp(i)$ random; (ii) the *random z-z exchange* model with $J_\perp(i)=1$, $\forall i$ and $J_z(i)$ random; (iii) the *random exchange* XXZ antiferromagnet for which $J_\perp(i)=J_z(i)$ and are all random numbers.

For the AF XXZ spin-$\frac{1}{2}$ chain, it has been shown by Doty and Fisher[6] that disorder is relevant and that any amount of randomness destroys the quasilong range order and drives the system from a line of pure fixed points to an infinite randomness fixed point (IRFP).[7] The situation for higher spins $S>\frac{1}{2}$ is more complicated since it depends[8] on the parity of $2S$ and some issues are still under debate.[9,10] Regarding the thermodynamic properties of the random spin-$\frac{1}{2}$ XXX antiferromagnet, a real space renormalization group (RSRG) scheme, introduced first by Ma, Dasgupta, and Hu[11] leads to a number of analytical results. In particular, independent of the initial distribution $\mathcal{P}(J)$ of couplings the low energy properties at the IRFP are characterized by a dynamical exponent $z=\infty$ and a GS which consists of a tensorial product of randomly long-range coupled dimers, the so-called *random-singlet phase* (RSP).[7] In such a phase, the disorder averaged spin-spin correlation function is dominated by strongly correlated pairs and is therefore slowly decreasing, as a power-law

$$C^{\alpha}_{\mathrm{avg}}(r) = \overline{\langle S_i^{\alpha} S_{i+r}^{\alpha} \rangle}_{\mathrm{GS}} \propto \frac{(-1)^r}{r^{\eta_{\mathrm{RSP}}}}, \tag{4}$$

where $\eta_{\mathrm{RSP}}=2$ for all spin components α ($\overline{\cdots}$ denotes the average over the disorder and the sites i). On the other hand, in the RSP the *typical* correlations decay faster (i.e., with a stretched exponential) than the *average* correlations. These analytical predictions, that we will recall in greater detail in Sec. II, have been tested numerically several times using different methods, e.g., Lanczos exact diagonalisation (ED);[12] free-fermions ED;[5,13,14] numerical RSRG.[16] For strong enough disorder, such finite size systems computa-

tions were in good agreement with the expected RSP universal behavior [Eq. (4)]. However, a recent density matrix renormalization group (DMRG) calculation[18] for chains (with free boundary conditions) defined by Eq. (3) with weak randomness in the planar exchanges caused a debate,[19] which we intend to settle in this paper. Indeed, the conclusions of the DMRG simulations presented in Ref. 18 on systems up to 400 spins, quite similar to a previous one using smaller systems,[20] disagree with the IRFP scenario in so far as a dependence of the exponent η upon Δ and the disorder strength was claimed. In this paper, we intend to shed more light on this disorder induced phenomena in finite size (FS) random quantum spin-$\frac{1}{2}$ chains and demonstrate convincingly via numerical studies of several related models defined by Eq. (3) the consistency of FS effects and the IRFP scenario.

The RSRG scheme is expected to be asymptotically exact, but FS effects cannot be negligible, especially for weak disorder, i.e., far away from the IRFP. Indeed, one can show that the RG flow toward the IRFP is controlled by a crossover characterized by a length scale ξ which is disorder dependent and diverges when the disorder strength is approaching zero. Such a crossover from pure to random critical behavior is very common in disordered systems and is always relevant, in experiments as well as in numerical studies, when the disorder is not too strong and the length scales that can be explored are not too large. A good understanding of the order of magnitude of the crossover length scale, in particular its scaling behavior in dependence of the disorder strength, is therefore necessary in order not to be misled by the mere appearance of the experimental and/or numerical data (cf. Refs. 18 and 19).

Our purpose here is to study crossover effects for various 1D spin-$\frac{1}{2}$ disordered models and to extract the relevant (disorder dependent) lenght scale which controls such a phenomenon. Already mentioned by two of us in Ref. 19, this disorder induced behavior is presented in greater details here and is illustrated through large scales numerical calculations. Moreover, a nontrivial connection with the localization of particles in a 1D disordered media is presented and only one relevant disorder dependent lenght scale is found to control crossover as well as localization phenomena. The rest of the paper is organized as follows. In Sec. II, we first recall the analytical predictions of the RSRG scheme. Then, using the bosonization study of the weakly disordered spin-$\frac{1}{2}$ chain,[6] we establish a disorder-dependent length scale which is the localization length of the related problem of disordered particles in 1D.[21] In Sec. III, we present the free-fermions ED results for the spin-spin correlation functions for various disorder strengths for system sizes (with periodic boundary conditions) up to 4096 sites. The crossover length scale, which emerges naturally from the data analysis, is studied as a function of the strength of the disorder and compared with the localization length extracted from spin stiffness calculations. The Ising part of the Hamiltonian [Eq. (3)] has also been included and investigated via quantum Monte Carlo simulations, using the stochastic series expansion (SSE) method. Section IV is devoted to SSE calculations performed at very low temperatures for the random exchange XXX model and the random planar exchange model. First a brief explanation of the method is given and some technical issues about equilibration and GS convergence are discussed; then results for spin-spin and string correlation functions are shown. Finally in Sec. V, we give a summary and some concluding remarks.

II. ANALYTICAL PREDICTIONS

A. Real space renormalization group results

The RSRG method, introduced originally by Ma, Dasgupta, and Hu for the random exchange XXX spin-$\frac{1}{2}$ chain[11] has been developed and studied in an exhaustive way by Fisher[7] for more general random exchange XXZ Hamiltonians. The basic ingredient of this decimation procedure is a successive decrease of the energy scale via a successive decimation of the strongest couplings in the chain.

In the limit of infinite system size, Fisher has demonstrated the existence of a fixed point for the the distribution of the effective couplings, independent of the initial distribution, which is given by

$$\mathcal{P}_0(\tilde{J}) \propto \tilde{J}^{-1+\delta^{-1}}, \quad \delta \to \infty. \tag{5}$$

The IRFP, characterized by such a broad distribution, is attractive for any amount of randomness in the case of spins-$\frac{1}{2}$ and the RSP, discussed in Sec. I, describes the GS. At the critical point, the energy and length scales are related via

$$\ln \Delta_\epsilon \sim -\sqrt{L} \tag{6}$$

and as a consequence, the dynamical exponent z is infinite. Concerning the correlation functions, the average and typical values behave quite differently since rare events control the physics [see Eq. (4)]. The average correlation function is dominated by long-range paired singlet and takes the following expression, independently of the direction (transverse or longitudinal)

$$C_{\text{avg}}(r) \propto \frac{(-1)^r}{r^2}. \tag{7}$$

Another quantity, which measure an hidden order is the *string correlation function*, defined in the GS at distance r by

$$S(r) = \frac{2^{r+1}}{L} \sum_{i=1}^{L} \langle S_i^z S_{i+1}^z \cdots S_{i+r}^z \rangle_{\text{GS}}. \tag{8}$$

At the IRFP, the disorder averaged expectation value $S_{\text{avg}}(r)$ is expected to decrease as a power law, with a well-defined exponent,[22]

$$S_{\text{avg}}(r) = \overline{S(r)} \propto \frac{(-1)^r}{r^{2-\phi}}, \tag{9}$$

$\phi = (1+\sqrt{5})/2$ being the golden mean.

Whereas this real space procedure provides predictions for the thermodynamic limit, it does not capture FS effects. However, in order to give good interpretations of numerical results, the understanding of FS effects is crucial. This is what we are striving for here, using the bosonization treatment of the random chain.

B. Bosonization of the random chain: Emergence of a disorder-dependent length scale

In this part, we summarize previous results obtained using bosonization techniques.[6,21] The XXZ spin-$\frac{1}{2}$ chain can be mapped using the Jordan-Wigner transformation (see Sec. III) into a spinless interacting fermions problem in 1D. The low-energy excitations around the Fermi points can be considered in terms of bosonic fields and the resulting Hamiltonian describes a Luttinger liquid.[23] It is characterized by a set of Δ-dependent *Luttinger liquid parameters* which are the velocity of excitations u and the parameter K, given by

$$u(\Delta) = \frac{\pi}{2}\frac{\sin(\mu)}{\mu}, \quad K(\Delta) = \frac{\pi}{2(\pi-\mu)}. \tag{10}$$

Several types of quenched randomness added to the pure XXZ model have been studied by Doty and Fisher.[6] They found, for random perturbations that preserves the XY symmetry, a critical behavior which belongs to the universality class of the Giamarchi-Schulz transition for 1D bosons in a random potential.[21] Let us define the disorder strength $\mathcal{D}$ by

$$\mathcal{D}_{\perp,z} = \overline{(J_{\perp,z}(i))^2} - (\overline{J_{\perp,z}(i)})^2. \tag{11}$$

More precisely, for the random planar exchange model $\mathcal{D}=\mathcal{D}_\perp$, for the random z-z exchange model, $\mathcal{D}=\mathcal{D}_z$ and for the random exchange XXZ model, since the randomness is isotropic $\mathcal{D}=\mathcal{D}_\perp=\mathcal{D}_z$. For a weak random perturbation added to the planar exchange, the renormalization under a change of length scale $l=\ln L$ is

$$\frac{\partial \mathcal{D}}{\partial l} = (3-2K)\mathcal{D}. \tag{12}$$

Therefore, if $K<3/2$ (i.e.) $-\frac{1}{2}<\Delta<1$) the disorder is a relevant perturbation and the phase is the RSP. The renormalization flow toward the IRFP is controlled by a length scale which emerges from Eq. (12),

$$\xi^*(\mathcal{D}) \sim \mathcal{D}^{-[1/(3-2K)]}. \tag{13}$$

For the random exchange XXX model, the random perturbation added to the operator $S_i^z S_{i+1}^z$ is marginally irrelevant and therefore the exponent $1/(3-2K)=\frac{1}{2}$ for $\Delta=1$ is expected to have small logarithmic corrections.[24]

The length scale ξ^* is called the localization length since in the fermionic language, the transition at $\mathcal{D}>0$ is a localization transition.[21,25] Such a metal-insulator transition driven by the disorder is characterized for instance, by the vanishing of the zero temperature Drude weight (also called the charge stiffness or the spin stiffness in the case of the spin-1/2 XXZ model) $\forall \mathcal{D}>0$ in the thermodynamic limit. Previous numerical studies have checked this effect on transport properties in the case of interacting spinless fermions in a random potential using ED (Ref. 26) or equivalently in the case of the XXZ chain in a random magnetic field.[27,28] For the simpler model of noninteracting fermions with random hopping, mapped into the random exchange XX spin chain, very large scale numerical simulations have been carried out on systems up to 2048 sites.[29] Using the scaling law for the spin stiffness

$$\rho_s(L,\mathcal{D}) = g(L/\xi^*(\mathcal{D})), \tag{14}$$

the localization length has been precisely studied and agrees perfectly with Eq. (13) for weak disorder (see Sec. III C and Figs. 4 and 5). Regarding the low-energy effective theory predicted by some bosonization calculations, there is only one relevant length scale which emerges from it, i.e., the localization length $\xi^*(\mathcal{D})$. Based on numerical calculations performed over FS clusters for various disorder strengths, the next sections are dedicated to the study of the disorder dependence of the crossover length scale and its comparison with the localization length.

III. EXACT DIAGONALIZATION STUDY AT THE XX POINT

A. Free fermions representation

Let us consider the 1D XX spin-$\frac{1}{2}$ model with random exchange couplings $J_\perp(i)$. This quantum problem is governed by the following lattice Hamiltonian:

$$\mathcal{H}^{XX}_{\text{random}} = \sum_{i=1}^{L} [J_\perp(i)(S_i^x S_{i+1}^x + S_i^y S_{i+1}^y)]. \tag{15}$$

We impose periodic boundary conditions, $\mathbf{S}_{L+1}=\mathbf{S}_1$. It is well known that this spin problem can be mapped into a free spinless fermions model via the Jordan-Wigner transformation: $S_j^z = 1/2 - n_j$, and $S_j^+ = c_j e^{i\pi\sum_{l=1}^{j-1} n_l}$. The c_j satisfy fermionic commutation relations, $\{c_i^\dagger, c_j\}=\delta_{ij}$, and $n_j=c_j^\dagger c_j$ is the number of fermions (spin down) at the j-site. The Hamiltonian can then be written as

$$\mathcal{H}^{XX}_{\text{random}} = \sum_{i=1}^{L-1}\left[\frac{J_\perp(i)}{2}(c_i c_{i+1}^\dagger + \text{h.c.})\right] + \frac{J_\perp(L)}{2} e^{i\pi\mathcal{N}}(c_L c_1^\dagger + \text{h.c.}), \tag{16}$$

where h.c. is the Hermitian conjugate and $\mathcal{N}=\sum_{i=1}^{L} n_i$ is the number of fermions in the system. In the nonrandom case, the solution of the problem via a Fourier transformation is trivial[30] because of the translational invariance. But in the random system, this symmetry is broken and we have to solve numerically a random matrix problem. The way to obtain the correlation functions is straightforward and has already been explained in several previous works;[5,13,15,30] it amounts to a numerical calculation of the eigenvectors of a $L\times L$ band matrix and then the evaluation of a $(r-1)\times(r-1)$ (resp. 2×2) determinant in order to compute the transverse (resp. longitudinal) spin-spin correlation function at distance r $C^x(r)$ (resp. $C^z(r)$). We can note that in the same way, the string correlation functions can also be obtained.[13]

B. Numerical results for the spin-spin correlation functions: Crossover effects

In order to study the crossover as a function of the disorder strength, we have chosen the following W-dependent flat bond distribution

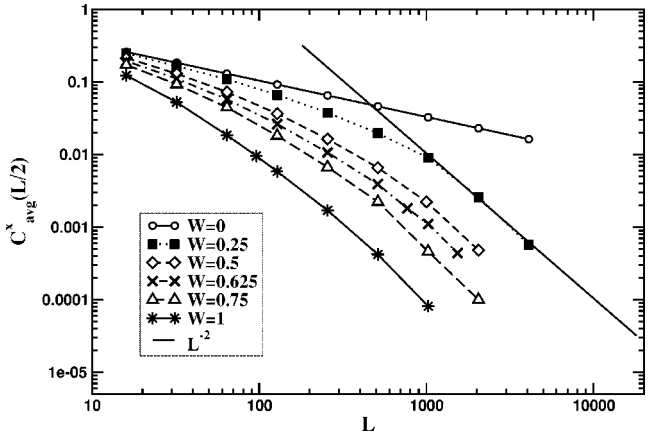

FIG. 1. Averaged correlation function $C^x_{\rm avg}(L/2)$ as a function of the system size L on a log-log scale for $W=0$, 0.25, 0.5, 0.625, 0.75, 1.0 (from top to bottom). The data are averaged over 50 000 samples for $L\leqslant 1024$, 3000 for $L=2048$ and 500 for $L=4096$, the statistical errors are smaller than the symbol sizes. The data for the pure system ($W=0$) follow $C^x(L/2)\propto L^{-1/2}$, the full line with slope −2 is the expected asymptotic behavior according to the IRFP scenario.

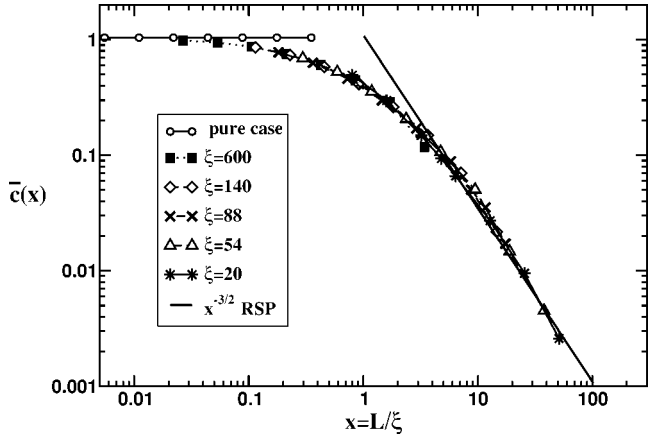

FIG. 2. Scaling plot according to Eq. (21) of the data shown in Fig. 1 with $\xi=600,140,88,54,20$ for $W=0.25$, 0.5, 0.625, 0.75, and 1.0, respectively. The symbols are identical to Fig. 1.

$$\mathcal{P}(J_\perp)=\begin{cases}\dfrac{1}{2W} & \text{if } J_\perp\in[1-W,1+W]\\ 0 & \text{otherwise.}\end{cases} \tag{17}$$

The disorder strength, defined by Eq. (11), is $\mathcal{D}=W^2/3$ and we define δ as the variance of the random variable $\ln J_\perp(i)$ by

$$\delta^2=\overline{(\ln J_\perp(i))^2}-(\overline{\ln J_\perp(i)})^2 \tag{18}$$

which is related to W according to

$$\delta=\sqrt{1-\frac{1-W^2}{4W^2}\left[\ln\left(\frac{1+W}{1-W}\right)\right]^2}. \tag{19}$$

We note that for weak disorder $W\ll 1$, $\delta\sim\sqrt{D}$. In order to reduce statistical errors and boundary effects we have used the PBC and computed the bulk correlation function in the transverse direction at midchain,

$$C^x\left(\frac{L}{2}\right)=\frac{2}{L}\sum_{i=1}^{L/2}\langle S_i^x S_{i+(L/2)}^x\rangle_{\rm GS} \tag{20}$$

for several system sizes ($L=2^q, q=1,\ldots,12$) and disorder strengths ($W=0.25,0.5,0.625,0.75,1$). The data for $C^x(L/2)$ were computed for each individual sample using standard routines and then averaged over the disorder. The number of disorder configurations was more than $5\cdot 10^4$ for $L\leqslant 1024$ and at least 500 for the largest size and weakest randomness ($L=4096, W=0.25$). In Fig. 1, we show the average bulk correlation function $C^x_{\rm avg}(L/2)=\overline{C^x(L/2)}$ for different disorder strengths. We observe that for small system sizes the slope of $C^x(L/2)$ versus L in a log-log plot is much smaller than 2, the value that one would expect form the IRFP scenario. But when L increases one observes a crossover, as reported in Ref. 19, from an apparently nonuniversal behavior with a W-dependent power law exponent $\eta(W)$ for small sizes to a universal behavior with $C^x_{\rm avg}(L/2)\sim L^{-2}$ for $L\to\infty$, as predicted by the RSRG.[7] Such a behavior suggests the existence of a disorder-dependent crossover length scale ξ which controls the crossover from the pure (instable) fixed point to the IRFP which is attractive, even for weak disorder. Defining the dimensionless parameter $x=L/\xi$, one can identify three different regimes:

(i) For $x\ll 1$, the critical behavior of the pure system [$J_\perp(i)=$constant] is dominant, with an exponent $\eta(W)=1/2$.

(ii) For $x\gg 1$, we are in the asymptotic regime where the predictions of the RSRG are recovered, in particular $\eta(W)=\eta_{\rm RSP}=2$.

(iii) For $x\sim 1$ we are in the crossover regime with a W- and L-dependent effective (FS) exponent $\eta(W)$.

Consequently, we expect the following scaling form:

$$C^x_{\rm avg}\left(\frac{L}{2}\right)=L^{-1/2}\tilde{c}(L/\xi), \tag{21}$$

where the scaling function $\tilde{c}(x)$ is constant in the regime (i), and $\tilde{c}(x)\to x^{-3/2}$ in the regime (ii). In Fig. 2, the scaling plot following Eq. (21) is shown for the data of Fig. 1. $\xi(W=1)$ has been chosen such that the crossover region (iii) is centered around $x\simeq 1$ and the other estimates have been adjusted in order to give the best data collapse.

C. The crossover length scale as a localization length

In this part, the dependence of the crossover length scale on the disorder strength is studied. A comparison with the localization length ξ^*, calculated using the spin stiffness of the random exchange XX chain, is also presented. Figure 3 shows a plot of ξ vs the disorder parameters $\mathcal{D}$ and δ. As expected one can observe a singular behavior for $\mathcal{D}$ or $\delta\to 0$. More precisely, we observe in Fig. 3(a) that for sufficiently weak disorder (typically for $\mathcal{D}<0.1$), the crossover length scale is well fitted by a power-law: $\xi(\mathcal{D})\propto\mathcal{D}^{-\gamma}$ with an exponent $\gamma=1\pm 0.1$, in good agreement with the localization length exponent predicted by Eq. (13) which gives $1/(3$

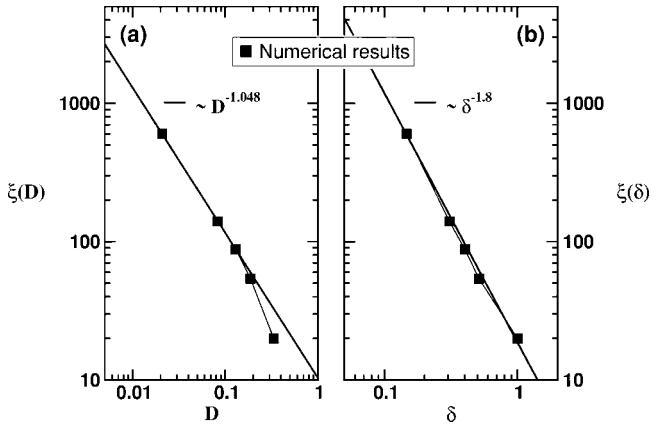

FIG. 3. Disorder dependence of the crossover length scale ξ of the random XX chain. The full squares are the numerical estimates from the data collapse in Fig. 2 and full lines are fits. (a) In function of the disorder parameter $\mathcal{D}$, a power law with an exponent −1.048 fits the data only for weak disorder whereas in (b), a fit $\xi(\delta) \sim \delta^{-1.8}$ works for the entire range of disorder strength studied here.

$-2K)=1$ at the XX point. For stronger disorder, a deviation from the power-law is observed. On the other hand, $\xi(\delta)$ shown in Fig. 3(b), can be fitted by a power-law $\xi(\delta) \propto \delta^{-\Phi}$, with $\Phi=1.8\pm0.2$ for the whole range of randomness studied here.

It is instructive to compare the crossover length scale ξ with the localization length ξ^*, extracted from the numerical calculation of the spin stiffness of the random exchange XX chain (for more details about this calculation, see Ref. 29). While the transport properties of random spin chains are not the purpose of this paper,[31] we mention here some results that two of us obtained by ED performed on the random exchange XX chain.[29] The spin stiffness ρ_s which measures the magnetization transport along the ring is calculated in the GS as the second derivative of the GS energy per site with respect to a twist angle φ applied at the boundaries using the so-called *twisted boundary conditions*,[32] and taking the limit $\varphi \to 0$. For the same model [Eq. (15)] studied in this section and for systems sizes going from 8 to 2048 sites, ρ_s has been calculated by ED techniques for several disorder strengths (from $W=0.025$ to $W=1$) and averaged over a very large number of samples (from 10^5 for the smallest sizes to 500 for the largest).

The stiffness ρ has dimension of inverse (length$^{d-2} \times \xi_\tau$), where ξ_τ is the correlation length in the imaginary time direction.[33] In our case $\xi_\tau \sim \exp(A\xi^{1/2})$, which is one manifestation of the IRFP that dominates the critical behavior of the random XX chain, and $\xi=L$ for a finite system at criticality we expect ρ to scale as $\ln \overline{\rho_S(L)} \sim -\sqrt{L}$. Combining this with Eq. (14) we show in Fig. 4 a scaling plot of $-(\ln g(L/\xi^*))^{-1}$ which displays the same features as Fig. 2. Indeed, for $L \ll \xi^*$, the pure behavior is observed with a stiffness $\rho_S \simeq 1/\pi$,[34] and for $L \gg \xi^*$, the IRFP behavior is recovered with $\ln g(L/\xi^*) \sim -(L/\xi^*)^{0.5}$; the regime where $L \sim \xi^*$ being a crossover regime.

The localization length $\xi^*(W)$ has been estimated for different values of the disorder strength (note that the computational demand for calculating the stiffness is substantially

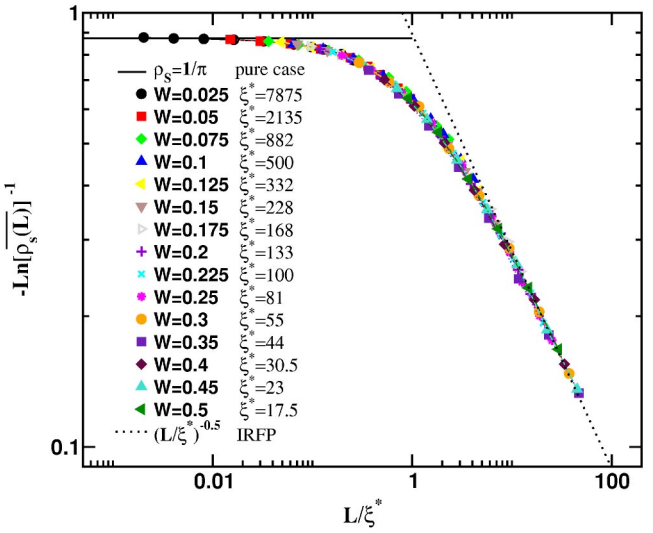

FIG. 4. Inverse logarithm of the disorder averaged spin stiffness plotted for several box sizes W specified on the plot. All the curves are collapsed since a rescaling of the x-axis has been done, providing an universal curve as a function of L/ξ^* The W-dependent localization length ξ^* has been calculated for each disorder strength, as indicated on the plot, in order to give the best data collapse. The full line stands for the pure case and the dotted one is for the IRFP behavior.

smaller than the one for the correlation function,[35] for which reason we could compute more data points) and is shown in Fig. 5 versus the disorder parameter. We see clearly that the behavior of the crossover length ξ as a function of the disorder strength (see Fig. 3) is exactly analogous to the one of the localization length ξ^*. Indeed, for $\mathcal{D} \ll 1$, the bosonization result Eq. (13) agrees with numerical results, as shown in Fig. 5(a), and for stronger disorder we observe the same deviation as in $\xi(\mathcal{D})$. Figure 5(b) gives us the confirmation that for strong disorder Eq. (13) has to be replaced by

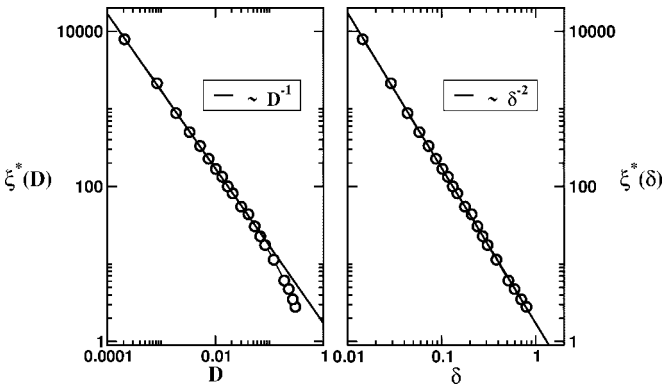

FIG. 5. Disorder dependence of the localization length ξ^* of the random XX chain calculated using the scaling of the stiffness [Eq. (14)]. (a) In the function of the disorder parameter $\mathcal{D}$, the expected power-law Eq. (13) with an exponent equal to −1 is in perfect agreement with numerical data (open circles) which can be fitted for weak disorder, with an exponent equal to -1 ± 0.01. (b) In the function of the other disorder parameter δ, the numerical data (open circles) are perfectly described by a power-law, for the entire range of disorder, with an exponent equal to -2 ± 0.02.

$$\xi^*(\delta) \sim \delta^{-\Phi}. \tag{22}$$

Since for weak disorder $\delta \sim \sqrt{\mathcal{D}}$, we expect $\Phi = 2/(3-2K)$ which works perfectly for the entire range of disorder considered here, as shown in Fig. 5(b).

Let us summarize our results that we obtained so far for the random exchange XX chain. With ED calculations we studied the crossover that controls the renormalization flow starting from a system with a finite disorder to an infinite disorder fixed point. As predicted by RSRG and bosonization calculations, the IRFP is attractive for any amount of initial disorder and the crossover length scale ξ is well described by a power-law, diverging like $\mathcal{D}^{-\gamma}$. Moreover, the exponent γ has been identified to be identical with the localization length exponent occurring in $\xi^*(\mathcal{D}) \sim \mathcal{D}^{-[1/(3-2K)]}$. While the parameter $\mathcal{D}$ is suitable to quantify the divergence near 0, we have found the parameter δ, Eq. (18), to be a better candidate to describe localization and/or crossover behaviors for any strength of randomness: $\xi(\delta) \sim \xi^*(\delta) \propto \delta^{-\Phi}$ with $\Phi = 2/(3-2K)$.

IV. QUANTUM MONTE CARLO STUDY

A. The SSE method

The quantum Monte carlo SSE method has been described as a loop algorithm in detail by one of us in Ref. 36. More recently the concept of directed loop has been developed[37–39] and the efficiency of such an algorithm has been demonstrated for several models, in particular for the XXZ model, defined by Eq. (1). We start from the general random-exchange XXZ Hamiltonian (3) that we can rewrite as a sum over diagonal and off-diagonal operators

$$\mathcal{H}^{XXZ}_{\text{random}} = -\sum_{b=1}^{L} [J_z(b) H_{1,b} - J_\perp(b) H_{2,b}],$$

where b denotes a bound connecting a pair of interacting spins $(i(b), j(b))$.

$$H_{1,b} = C - \Delta S^z_{i(b)} S^z_{j(b)} \tag{23}$$

is the diagonal part and the off-diagonal part is given by

$$H_{1,b} = \frac{1}{2}[S^+_{i(b)} S^-_{j(b)} + S^-_{i(b)} S^+_{j(b)}], \tag{24}$$

in the basis $\{|\alpha\rangle\} = \{|S^z_1, S^z_2, \ldots, S^z_L\rangle\}$. The constant C which has been added to the diagonal part ensures that all nonvanishing matrix elements are positive. The SSE algorithm is based on Taylor expanding the partition function $Z = \text{Tr}\{e^{-\beta \mathcal{H}^{XXZ}_{\text{random}}}\}$ up to a cutoff $\mathcal{M}$ which is adapted during the simulations in order to ensure that all the elements of order higher than $\mathcal{M}$ in the expansion do not contribute. So,

$$Z = \sum_\alpha \sum_{S_\mathcal{M}} \frac{\beta^n (\mathcal{M}-n)!}{\mathcal{M}!} \langle \alpha | \prod_{i=1}^{\mathcal{M}} J_{a_i}(b_i) H_{a_i,b_i} | \alpha \rangle, \tag{25}$$

where $S_\mathcal{M}$ denotes a sequence of operator indices

$$S_\mathcal{M} = [a_1, b_1], [a_2, b_2], \cdots [a_\mathcal{M}, b_\mathcal{M}] \tag{26}$$

with $a_i = 1, 2$ corresponds to the type of operator (diagonal or not) and $b_i = 1, 2, \ldots, L$ is the bond index. Note that $J_1(b) = J_z(b)$ and $J_2(b) = J_\perp(b)$. A Monte Carlo configuration is therefore defined by a state $|\alpha\rangle$ and a sequence $S_\mathcal{M}$. Of course, a given operator string does not contain $\mathcal{M}$ operators of type 1 or 2, but only n; so in order to keep constant the size of $S_\mathcal{M}$, $\mathcal{M}-n$ unit operators $H_{0,0} = 1$ have been inserted in the string, taking into account all the possible ways of insertions. The starting point of a simulation is given by a random initial state $|\alpha\rangle$ and an operator string containing $\mathcal{M}$ unit operators $[0,0]_1, \ldots, [0,0]_\mathcal{M}$. The first step is the *diagonal update* which consists in exchanging unit and diagonal operators at each position p $[0,0]_p \leftrightarrow [1,b_i]_p$ in $S_\mathcal{M}$ with Metropolis acceptance probabilities

$$P_{[0,0]_p \to [1,b]_p} = \min\left[1, \frac{J_z(b) L \beta \langle \alpha(p) | H_{1,b} | \alpha(p) \rangle}{\mathcal{M}-n}\right], \tag{27}$$

$$P_{[1,b]_p \to [0,0]_p} = \min\left[1, \frac{\mathcal{M}-n+1}{J_z(b) L \beta \langle \alpha(p) | H_{1,b} | \alpha(p) \rangle}\right]. \tag{28}$$

During the "propagation" from $p = 1$ to $p = \mathcal{M}$, the "propagated" state

$$|\alpha(p)\rangle \sim \prod_{i=1}^{p} H_{a_i,b_i} |\alpha\rangle \tag{29}$$

is used and the number of nonunit operators n can varies at each index p. The following step is the *off-diagonal update*, also called the *loop update*, carried out at n fixed. Its purpose is to substitute $[1,b_i]_p \leftrightarrow [2,b_i]_p$ in a cluster-type update, i.e., with the operators forming closed loops. Such a construction has already been discussed in detail elsewhere.[37] A very efficient directed loop implementation can be used and for $\Delta \in [0,1]$ it has been shown that during the construction of the loop, back-tracking processes can be avoided. At the SU(2) AF point, the algorithm is deterministic because we can build all the loops in a unique way. So, for $\Delta = 1$, all the loops are updated independently of each other with probability 1/2. For $\Delta \neq 1$ the construction of the loop depends on some well defined probabilities[37] at each time a non unit operator is encountered in the loop building.

One MC step is consists of *diagonal* updates at all possible locations in the index sequence, followed by a number of loop updates (the number adjusted so that the average number of operators changes is comparable to the total number of operators). Before starting the measurement of physical observables, one has to perform equilibration steps, notably necessary to adapt the cutoff $\mathcal{M}$.

B. Convergences issues

The precise determination of physical observables using quantum Monte Carlo suffers obviously from statistical errors since the number of MC steps is finite. As we deal with disordered spin chains, the sample to sample variation is another source of errors. Moreover, the calculation of GS ex-

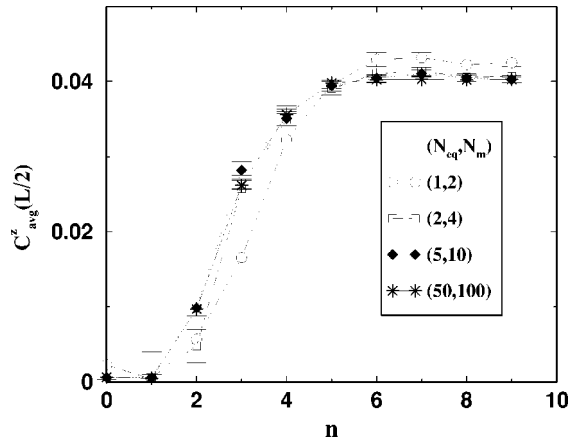

FIG. 6. Test for the convergence of the disorder averaged longitudinal correlation function calculated for a the random exchange XXX chain at $W=0.5$ with 16 sites. Results, averaged over 10^3 samples, are for a different number of MC steps (N^{eq}, N_m) as shown on the plot. The β-doubling scheme has been used with inverse temperatures $\beta_n=2^n$, with n used here for the x-axis.

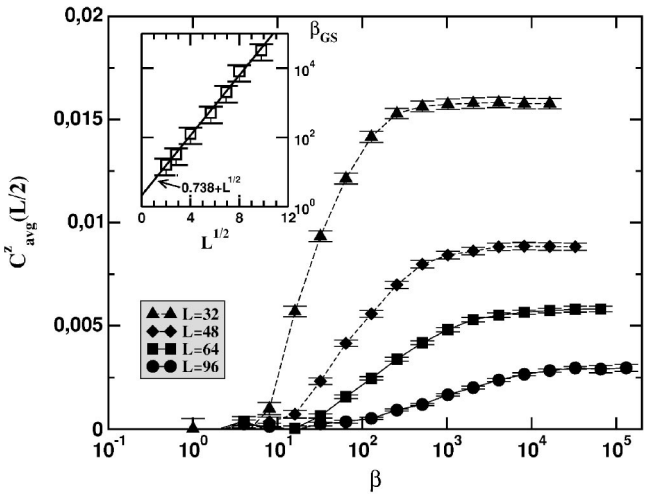

FIG. 7. Test for the GS convergence of $C^z_{avg}(L/2)$, defined by Eq. (31), versus the inverse temperature β. SSE calculations performed on the random exchange XXX model for $W=0.6$ using the β-doubling scheme with $(N_{eq},N_m)=(50,100)$. Averaging has been done over 10^3 different samples and the results are shown for the 4 larger sizes $L=32$, 48, 64, and 96. In the inset, the GS inverse temperature β_{GS} (see the text for its definition) is plotted in a log scale versus the square root of system sizes. A linear fit is represented by the full line.

pectation values for a system close to an IRFP, where FS gap scale like $\ln \Delta_\epsilon \sim \sqrt{L}$, requires a very carefully numerical treatment. In order to avoid finite temperature effects and to ensure that we measure observables in the GS, we use the β-doubling scheme, developed in Ref. 40 and then used in Refs. 10 and 41. Such a scheme is a very powerful tool because it allows to reach extremely low temperatures rather rapidly *and* reduces considerably equilibration times in the MC simulation. The procedure is quite simple to implement and its basic ingredient consists in carrying out simulations at successive inverse temperatures $\beta_n=2^n$, $n=0,1,\ldots,n_{\max}$. Starting with a given sample at $n=0$ we perform a small number of equilibration steps N_{eq} followed by $N_m=2N_{eq}$ measurement steps. At the end of the measurement process, β is doubled (i.e., $n\rightarrow n+1$) and in order to start with an "almost equilibrated" MC configuration, the starting sequence used is the previous $S_{\mathcal{M}}$ doubled, i.e.,

$$S_{2\mathcal{M}}=[a_1,b_1],\ldots,[a_{\mathcal{M}},b_{\mathcal{M}}][a_{\mathcal{M}},b_{\mathcal{M}}],\cdots,[a_1,b_1]. \tag{30}$$

Such a scheme becomes very efficient at low temperature and for disordered systems, in which very small correlations may develop. It is for the moment the most efficient technique available to cancel remaining temperature effects although a zero-temperature SSE algorithm might be developed soon.[42] The next point concerns the number of equilibration and measurement steps that we have to perform. It is illustrated for an $L=16$ random exchange XXX chain with random bonds distributed according to Eq. (17) with $W=0.5$ in Fig. 6. Here the disorder averaged midchain longitudinal correlation function

$$C^z_{\text{avg}}\left(\frac{L}{2}\right)=\frac{2}{L}\sum_{i=1}^{L/2}\langle S^z_i S^z_{i+(L/2)}\rangle_{\text{GS}} \tag{31}$$

is plotted for different values of (N_{eq}, N_m). The averaging is done over 10^3 independent samples and we observe that when the temperature becomes low enough, even for a couple (N_{eq}, N_m) quite small, averaged values do not depend on the number of MC steps. As already mentioned in Refs. 10, 40, and 41 we conclude that the sample to sample variation produces larger error bars than statistical errors, even for a number of measurement steps $\leqslant 100$, and in the following we will use the β-doubling scheme with $(N_{eq},N_m)=(50,100)$ and a sufficiently large number of samples ($\geqslant 10^3$).

In order to make reliable predictions for the GS, very large β have to be reached. This is illustrated for the random exchange XXX model with disorder strength $W=0.6$ in Fig. 7, where $C^z_{\text{avg}}(L/2)$ is plotted vs β for different chain sizes L. We consider that the GS expectation value is obtained when there are no statistically significant differences between the results for $\beta_{\max}=2^{n_{\max}}$ and $\beta=2^{n_{\max}-1}$. More precisely, our GS convergence criterion is the following: the GS is considered reached if the expectation value is 98% of the saturation value. Note that using such a criterion, we can define a system size dependent temperature scale below which the thermal expectation values are indistinguishable from GS expectation values: $\beta_{\text{GS}}=2^{n_{\max}-1}\pm 2^{n_{\max}-2}$ and as shown in the inset of Fig. 7, we obtain for this quantity a FS scaling of the form $\ln \beta_{\text{GS}} \sim \sqrt{L}$ for $W=0.6$. Note that we have checked the validity of this scaling for all disorder strengths considered here. Such a scaling is not surprising since the FS gap also obeys to a similar law Eq. (6).

C. Spin-spin correlation functions of the random-exchange XXX model

After these careful checks of equilibration and temperature effects in our simulations, we can analyze the SSE re-

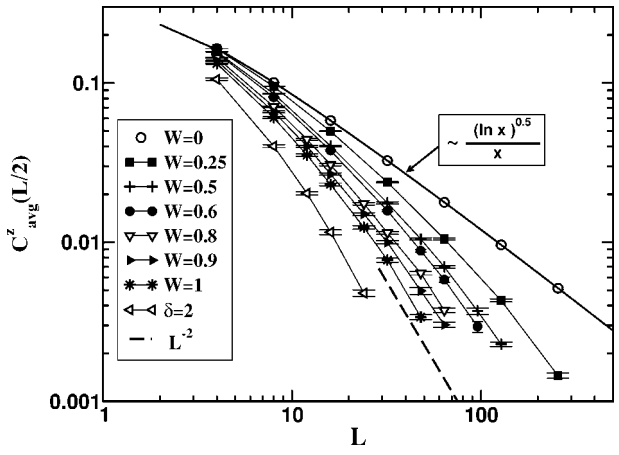

FIG. 8. Averaged longitudinal correlation function $C^z(L/2)$ for the random XXX model as a function of the system size L on a log-log scale for $W=0,0.25,0.5,0.6,0.8,0.9,1.0$ and $\delta=2$ (top to bottom). The data, computed in the GS using SSE method and β-doubling scheme, are averaged over more than 1000 samples. The data for the pure system ($W=0$, open circles) follow $C^z(L/2) \propto \sqrt{\ln(L)/L}$, the dashed line with slope -2 is the expected asymptotic behavior according to the IRFP scenario.

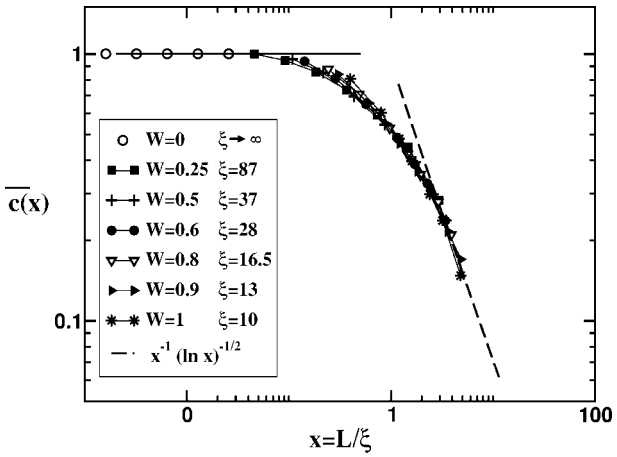

FIG. 9. Scaling plot according to Eq. (34) for the data of Fig. 8 with $\xi=87,37,28,16.5,13,10$ for $W=0.25,0.5,0.6,0.8,0.9$, and 1.0, respectively. The full line stands for the pure behavior and the dashed line is the expected asymptotic behavior according to the IRFP scenario.

sults obtained for the disorder averaged longitudinal spin-spin correlation $C^z_{\rm avg}$. In order to extract the bulk value, we compute this quantity at midchain and perform the averages along the chains and over random samples, according to Eq. (31). We consider in the following the random exchange XXX Hamiltonian

$$\mathcal{H}^{XXX}_{\rm RE} = \sum_{i=1}^{L} [J(i)(S^x_i S^x_{i+1} + S^y_i S^y_{i+1} + S^z_i S^z_{i+1}], \qquad (32)$$

with $J(i)$ random AF couplings taken from the W-dependent distribution Eq. (17). We have also used the more singular distribution $\mathcal{P}(J)=\delta J^{-1+\delta^{-1}}$ if $J \leqslant 1$ and 0 otherwise, with $\delta=2$. Such a distribution is, a priori, closer to the IRFP and therefore we expect the asymptotic behavior $C^z_{\rm avg}(L/2) \sim L^{-2}$ to become visible already for not too large system sizes. Indeed, this is what we can see in Fig. 8, where $C^z_{\rm avg}(L/2)$ is plotted versus L for different disorder strengths. The crossover phenomena, already mentioned for the random exchange XX case, is also clearly visible but from 16 sites the RSP behavior is recovered for the $\delta=2$ case. For weaker disorder, the asymptotic behavior is visible only for larger distances and an analysis analogous to the one we have performed for the XX chain is necessary in order to extract a disorder-dependent crossover length scale ξ. In the pure XXX case the exponent in Eq. (2) is $\eta_z=1$, but logarithmic corrections have to be taken into account[43]

$$C^z(r) \propto (-1)^r \frac{\sqrt{\ln r}}{r}, \qquad (33)$$

with which our numerical data for $W=0$ agree (see Fig. 8).

As in the XX case we expect a disorder dependent length scale ξ to govern the crossover from pure XXX behavior for $L \ll \xi$ to the asymptotic RSP behavior visible for $L \ll \xi$. Then $C^z(L/2)$ should obey the following scaling form:

$$C^z_{\rm avg}\left(\frac{L}{2}\right) = \frac{\sqrt{\ln L}}{L} \tilde{c}(L/\xi), \qquad (34)$$

with $\tilde{c}(x)$ a scaling function that is constant in the pure regime ($x \ll 1$) and proportional to $(x \ln^{1/2} x)^{-1}$ for $x \gg 1$ in order to reproduce the IRFP behavior $C^z_{\rm avg}(L/2) \propto L^{-2}$ for $L \gg \xi$. In Fig. 9, the scaling Eq. (34) is shown for the data of Fig. 8.[44] The W-dependent crossover lengths scale ξ was chosen for each value for W individually to obtain the best data collapse. $\xi(W=1)$ has been chosen such that the crossover regime is centered around $x \simeq 1$ (i.e., when the system size is of the same order of magnitude as the crossover length scale ξ). In comparison with the XX results (see Sec. III), the asymptotic behavior $C^z_{\rm avg} \sim L^{-2}$ sets in already for smaller system sizes. This observation is compatible with the fact that that the disorder dependent length scale defined in Eq. (13) diverges much slower at the XXX point ($\xi_{XXX} \propto \mathcal{D}^{-1/2}$), than at the XX point ($\xi_{XX} \propto \mathcal{D}^{-1}$).

The disorder dependence of the crossover length scale of the random exchange XXX model is shown in Fig. 10. For $D \to 0$ it diverges with a power law and for small disorder strengths, we can fit the data well by $\xi(\mathcal{D}) \sim \mathcal{D}^{-0.6\pm0.1}$ [see Fig. 10(a)]. As a function of δ the fit $\xi(\delta) \sim \delta^{-1.2\pm0.2}$ is working in the whole range of disorder strengths [see Fig. 10(b)].

The agreement of our numerical estimate of the exponent governing the divergence of the crossover lengths with the bosonization prediction for the localization length (0.6 ± 0.1 versus 0.5) is not as good as in the XX case but still acceptable within the error bars. These minor deviations might be due to small logarithmic corrections to formula (13). This is expected since the bosonization approach gives predictions for the random planar exchange model, whereas the random exchange case considered here is only qualitatively similar

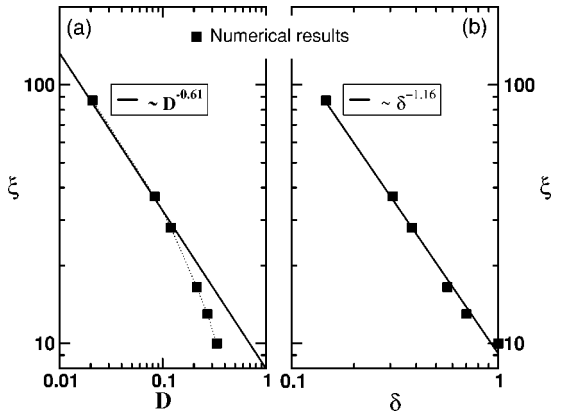

FIG. 10. Disorder dependence of the crossover length scale ξ of the random XXX chain. The full squares are the numerical estimates from the data collapse in Fig. 9. (a) In the function of the disorder parameter $\mathcal{D}$, the power law fit $\xi \sim \delta_W^{-0.61\pm0.1}$ works only for weak disorder whereas in (b), the fit $\xi \sim \delta_W^{-1.16\pm0.2}$ works for the entire range of disorder strength studied here.

because the randomness added to the Ising term is marginally irrelevant.[24]

D. String correlation function

The string correlation, Eq. (8), was introduced to measure hidden order in in integer spin chains where the ordinary spin-spin correlations vanish exponentially. In the RS phase the decay of the string correlation is expected to be described by a power law [see Eq. (9)], with a decay exponent of $\eta \sim 0.382$. It has been shown before[10,13] that the string correlation converges particularly quickly to the expected behavior.

In this section we begin by demonstrating yet another crossover effect in the random singlet phase: The RSRG calculation predicts that all components of the spin and string order correlations should decay with the same exponents although the underlying XXZ Hamiltonian is not rotationally invariant. This follows from the fact that the ground state of two S-$\frac{1}{2}$ spins coupled together by an interaction of the form

$$\mathcal{H} = J[S_1^x S_2^x + S_1^y S_2^y + \Delta S_1^z S_2^z] \tag{35}$$

is a rotationally invariant singlet, independently of the anisotropy Δ. So if all the spins really are bound pairwise in singlets, then the decay of different components of the correlation functions should be identical. However, at finite disorder strength, although the components are found to decay with the same exponents, the prefactors are different.[13] This is due to the fact that for finite disorder strength the strong bonds in the system are not necessarily surrounded by much weaker bonds, which leads to fluctuations in the singlet couplings. As the disorder strength is increased these fluctuations should diminish and true rotational invariance should be observed. Since the string order converges fairly quickly to the expected random singlet exponents it is a suitable quantity to use to illustrate this crossover behavior. In Fig. 11 the x and z components of the string order are shown for the XX chain with disorder parameters $W=0.5$, $W=1$, $\delta=10$. For

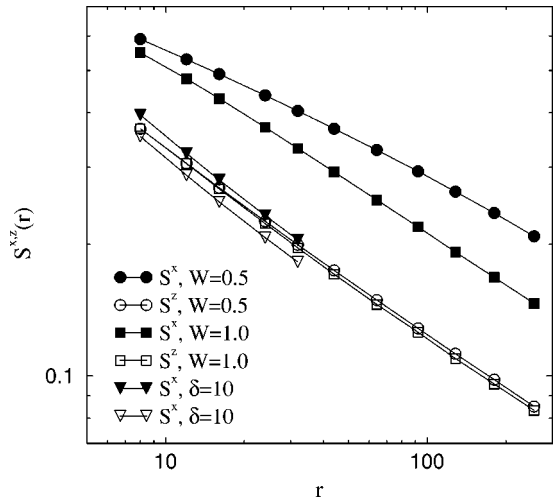

FIG. 11. Exact diagonalization results for the x and z components of the string order at disorder strengths $W=0.5$, $W=1$, and $\delta=10$.

flat disorder of strength $W=0.5$ the string correlation functions already decay with the expected RS exponent, but the two components are quite far from each other. Increasing the disorder strength to $W=1$ the two components approach each other, and for a power law distribution with $\delta=10$ they are within about 10% of each other. Increasing δ further brings them closer still, but it is necessary to use very high numerical precision to get reliable data.

In order to check the decay of the string order away from the XX point we again use the SSE method. Here we will use chains of length $L=256$ and go to sufficiently low temperatures to observe $T \to 0$ converged string correlations. In Fig. 12 the temperature effects are illustrated for an XX system at disorder strength $W=0.5$. In this case, it is possible to obtain $T \to 0$ converged results for all distances. For W close to 1, this would require prohibitively low temperatures, but it is

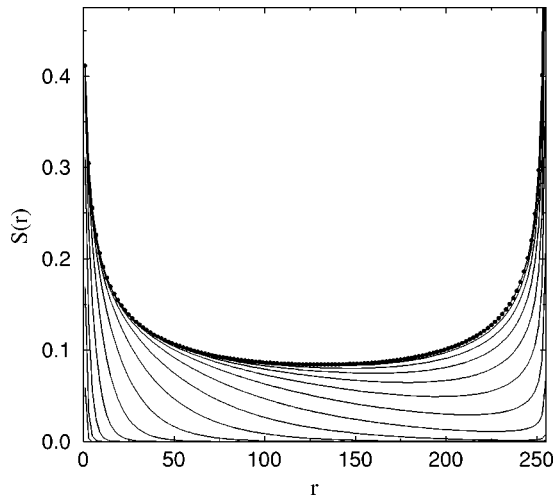

FIG. 12. SSE results for the string correlations of an $L=256$ XX system at $W=0.5$ calculated at inverse temperatures $\beta=2^n$ with $n=0,\ldots,15$. The $\beta=2^{15}$ results are shown with solid circles; the string correlations decrease with increasing temperature (decreasing n).

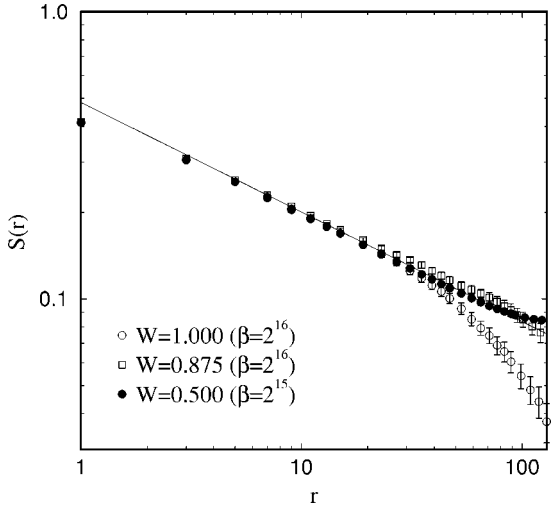

FIG. 13. SSE results for the string correlations of an $L=256$ XX system at different disorder strengths W, calculated at the inverse temperatures indicated in the figure. The straight line shows the $T=0$ RS power law.

still possible to obtain well converged results up to distances sufficiently long for observing the asymptotic RS behavior. Figure 12 also illustrates that the string correlations, unlike spin-spin correlations, are not symmetric with respect to $r=L/2$ in these periodic systems. From the definition, Eq. (8), it is clear that $S(r)$ cannot be symmetric unless the total magnetization $\Sigma_i S_i^z=0$. This is the case in the ground state, where indeed the symmetry is observed.

In Fig. 13 low-temperature results are shown at different W. Here deviations from the RS behavior due to temperature effects can be seen for $r\gtrsim 20$ when $W=1$, whereas deviations due to effects of the periodic boundaries (flattening out close to $r=L/2$) can be seen at $W=0.5$. In Fig. 14 we show similar results for the XXZ chain for two different combinations of the Ising anisotropy Δ and the disorder strength W. In both cases RS behavior can be observed over a significant distance range, before temperature or boundary effects become

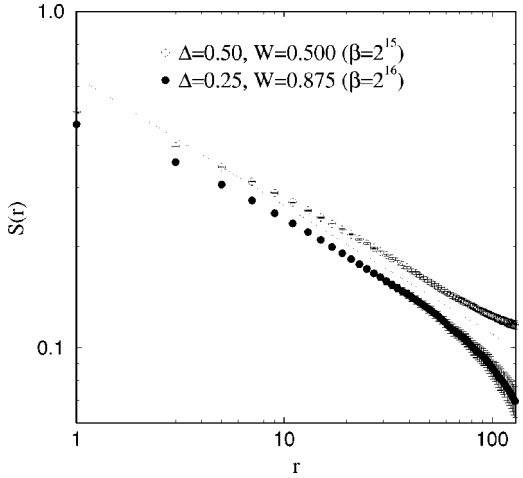

FIG. 14. SSE results for the string correlations of $L=256$ XXZ system at two combinations of Ising anisotropy Δ and disorder strength W. The line shows the $T=0$ RS behavior.

visible for $r\gtrsim 50$. The very good agreement with the RS exponent provides further evidence that the system indeed is in the RS phase for any anisotropy and disorder strength.

V. CONCLUSION

In this paper we have investigated numerically the spin-$\frac{1}{2}$ antiferromagnetic random-exchange XX and XXZ chains for varying disorder strength. Using exact diagonalization calculations at the XX point and quantum Monte Carlo SSE simulations for $\Delta\geqslant 0$ we studied the ground state spin-spin and string correlation functions for system sizes up to $L=4096$ for $\Delta=0$. With the SSE calculations for $\Delta>0$ we went up to $L=256$ and down to very low temperature, for instance we reached $\beta_{\max}=2^{17}$ at the random XXX point for $L=96$ and disorder strength $W=0.6$. We found clear evidences for the asymptotically universal behavior of the correlation functions as predicted by the RSRG analysis of Fisher.[7] The main issue of our work presented here consists in the detailed analysis of the RG flow from the pure instable line of XXZ fixed points toward the attractive infinite randomness fixed point. Indeed, as we have demonstrated, such a flow is controlled by a disorder dependent length scale ξ which diverges as the randomness approaches zero.[19] In our large scale numerical calculations we showed that the spin-spin correlation function is very sensitive to such crossover effects whereas the string order converges more rapidly to its asymptotic RS value. Nevertheless the string order also displays a crossover phenomena, visible not in the decay exponents as in the spin-spin case but rather in the prefactors.

The spin-spin correlation function as well as the stiffness display a clear crossover from the pure behavior to the IRFP behavior as predicted by the RSRG. The crossover length scale, extracted from numerical data, is shown to diverge as $\xi\sim\mathcal{D}^{-\gamma}$. Our estimates for the exponent $\gamma\approx 1.0$ agrees very well within the error bars with the localization length exponent calculated within an analytical bosonization approach.[6] However, as the bosonization approach is only valid for a disorder that is not too strong, our estimates for the crossover length scale $\xi(\mathcal{D})$ and for the localization length $\xi^*(\mathcal{D})$ both deviate (in a perfectly similar way) from the predicted behavior described by Eq. (13) when the disorder strength increases. For any strength of randomness, we found a better parameter to describe crossover as well as localization effects. Indeed, using the variance of the logarithm of the random couplings, δ given by Eq. (18), our estimates for the crossover length scale fits in the whole range of disorder strengths considered here very well the form $\xi(\delta)\sim\xi^*(\delta)\propto\delta^{-\Phi}$ with $\Phi=2/(3-2K)$. It would be interesting to check such a δ dependence of ξ or ξ^* also for $\Delta\neq 0$ or 1. The connection between crossover and localization effects has been clearly demonstrated here and has motivated further studies of the localization in 1D.[29]

Whereas the models we have studied are described by the IRFP for any strength of the disorder, several disordered magnetic systems require a critical value of randomness to display universal RSP features. For instance, gaped systems like the spin-1 chains or spin-$\frac{1}{2}$ n-legs ladders are not unstable with respect to the introduction of weak disorder and a

precise identification of the critical disorder $\mathcal{D}_c$ might be easier if one considers the divergence of ξ when the disorder strength approaches the critical value $\mathcal{D} \to \mathcal{D}_c$.

ACKNOWLEDGMENTS

N.L. would like to acknowledge stimulating discussions with E. Orignac. The work of N.L. and H.R. was financially supported by the Deutsche Forschungsgemeinschaft (DFG) and by the European Community's Human Potential Programme under Contract No. HPRN-CT-2002-00307, DYGLAGEMEM. A.W.S. acknowledges support from the Academy of Finland, Project No. 26175. P.H. acknowledges support from the Swedish Research Council and the Göran Gustafsson Foundation. A part of the simulations have been performed on parallel supercomputers at IDRIS (Orsay, France).

[1] H. Bethe, Z. Phys. **38**, 441 (1931).
[2] K. Hallberg, X. Q. G. Wang, P. Horsch, and A. Moreo, Phys. Rev. Lett. **76**, 4955 (1996).
[3] F. D. M. Haldane, Phys. Lett. **93A**, 464 (1983).
[4] N. D. Mermin and H. Wagner, Phys. Rev. Lett. **17**, 1133 (1966).
[5] F. Igloi, R. Juhász, and H. Rieger, Phys. Rev. B **61**, 11 552 (2000).
[6] C. Doty and D. S. Fisher, Phys. Rev. B **45**, 2167 (1992).
[7] D. S. Fisher, Phys. Rev. B **50**, 3799 (1994).
[8] G. Refael, S. Kehrein, and D. S. Fisher, Phys. Rev. B **66**, 060402(R) (2002); K. Damle and D. Huse, Phys. Rev. Lett. **89**, 277203 (2002); E. Carlon *et al.*, Phys. Rev. B **69**, 144416 (2004).
[9] K. Hida, Phys. Rev. Lett. **83**, 3297 (1999); K. Yang and R. A. Hyman, *ibid.* **84**, 2044 (2000); A. Saguia *et al.*, *ibid.* **89**, 117202 (2002).
[10] S. Bergkvist, P. Henelius, and A. Rosengren, Phys. Rev. B **66**, 134407 (2002).
[11] S. K. Ma, C. Dasgupta, and C.-K. Hu, Phys. Rev. Lett. **43**, 1434 (1979); C. Dasgupta and S.-K. Ma, Phys. Rev. B **22**, 1305 (1980).
[12] S. Haas, J. Riera, and E. Dagotto, Phys. Rev. B **48**, 13 174 (1993).
[13] P. Henelius and S. M. Girvin, Phys. Rev. B **57**, 11 457 (1998).
[14] Note that for the related model of the random transverse-field Ising model, free-fermions ED calculations have also confirmed the universal behavior on FS clusters ($L_{\max}=128$ spins), see Ref. 15.
[15] A. P. Young and H. Rieger, Phys. Rev. B **53**, 8486 (1996).
[16] T. Hikihara, A. Furusaki, and M. Sigrist, Phys. Rev. B **60**, 12 116 (1999).
[17] S. Todo, K. Kato, and H. Takayama, in *Computer Simulation Studies in Condensed-Matter Physics XI* (Springer-Verlag, Berlin, 1999), pp. 57–61.
[18] K. Hamacher, J. Stolze, and W. Wenzel, Phys. Rev. Lett. **89**, 127202 (2002).
[19] N. Laflorencie and H. Rieger, Phys. Rev. Lett. **91**, 229701 (2003).
[20] H. Röder, J. Stolze, R. Silver, and G. Müller, J. Appl. Phys. **79**, 4632 (1996).
[21] T. Giamarchi and H. J. Schulz, Phys. Rev. B **37**, 325 (1988).
[22] D. S. Fisher, Phys. Rev. Lett. **69**, 534 (1992); Phys. Rev. B **51**, 6411 (1995).
[23] For a review on Luttinger liquid, see H. J. Shulz, G. Cuniberti, and P. Pieri, *Fermi Liquids and Luttinger Liquids*, in *Field Theories for Low-Dimensional Condensed Matter Systems* (Springer, New York, 2000).
[24] E. Orignac (private communication).
[25] E. Abrahams, P. W. Anderson, D. C. Licciardello, and T. V. Ramakrishnan, Phys. Rev. Lett. **42**, 673 (1979).
[26] G. Bouzerar, D. Poilblanc, and G. Montambaux, Phys. Rev. B **49**, 8258 (1994).
[27] K. J. Runge and G. T. Zimanyi, Phys. Rev. B **49**, 15 212 (1994).
[28] L. Urba and A. Rosengren, Phys. Rev. B **67**, 104406 (2003); in this study, DMRG calculations have been performed on system up to 50 sites.
[29] N. Laflorencie and H. Rieger, Eur. Phys. J. B **40**, 201 (2004).
[30] E. Lieb, T. Schulz, and D. Mattis, Ann. Phys. (N.Y.) **16**, 407 (1961).
[31] For a study of dynamics and transport properties at nonzero frequency in random spin chains, see O. Montrunich, K. Damle, and D. Huse, Phys. Rev. B **63**, 134424 (2001).
[32] The twisted boundary conditions are given by $S^z_{L+1}=S^z_1$, $S^{\pm}_{L+1}=S^{\pm}_1 e^{\pm i\varphi}$.
[33] M. Wallin, E. S. Sørensen, S. M. Girvin, and A. P. Young, Phys. Rev. B **49** 12 115 (1994).
[34] This value $1/\pi$ is strictly valid in the thermodynamic limit, but the FS corrections are quite small $\propto L^{-2}$, see N. Laflorencie, S. Capponi, and E. S. Sørensen, Eur. Phys. J. B **24**, 77 (2001).
[35] For a sample of size L, we have to solve an eigenvalues problem twice on a $L\times L$ matrix to obtain the spin stiffness (once at $\varphi=0$ and once at $\varphi=\delta_\varphi$) whereas the evaluation of the mid-chain spin-spin correlation function requires to solve eigenvalues and eigenvectors problem on an $L\times L$ matrix and then requires us to calculate an $(L/2)\times(L/2)$ determinant.
[36] A. W. Sandvik, Phys. Rev. B **59**, R14 157 (1999).
[37] O. F. Syljuasen and A. W. Sandvik, Phys. Rev. E **66**, 046701 (2002).
[38] O. F. Syljuasen, Phys. Rev. E **67**, 046701 (2003).
[39] F. Alet, S. Wessel, and M. Troyer, cond-mat/0308495 (unpublished).
[40] A. W. Sandvik, Phys. Rev. B **66**, 024418 (2002).
[41] N. Laflorencie, D. Poilblanc, and A. W. Sandvik, Phys. Rev. B **69**, 212412 (2004).
[42] S. Todo (private communication).
[43] I. Affleck, D. Gepner, H. J. Schulz, and T. Ziman, J. Phys. A **22**, 511 (1989).
[44] Note that the fitting parameter $\lambda_0 \simeq 0.669$ was included in $\ln(L//\lambda_0)$ in order to get $\tilde{c}(x)\to 1$ when $x\to 0$.